

Wearable metamaterial for electromagnetic radiation shielding

Oriol Almirall, Raul Fernández-García and Ignacio Gil*

*Department of Electronic Engineering, Universitat Politècnica de Catalunya, Terrassa
Barcelona, Spain;*

*Correspondence: ignasi.gil@upc.edu

Acknowledgements

This work was supported by the Spanish Government MINECO under Project
TEC2016-79465-R.

Wearable metamaterial for electromagnetic radiation shielding

A novel wearable Frequency Selective Surface (FSS) created using fabric materials capable of blocking electromagnetic radiation around the frequency of 10.64 GHz (X Microwave frequency band) is presented in this paper. Two different unit cell shapes are tested: embroidered metal yarn squares and hexagons. A cotton fabric with permittivity 1.9 and thickness 0.4 mm is used as a substrate. The proposed design is validated by comparison of 3D electromagnetic simulations and measurements. The obtained results correspond to a maximum absorptivity of 99.23% at 10.63 GHz for the simulation using a square as unit cell, whereas the simulations using hexagons led to a maximum in absorptivity of 99.94% at 10.68 GHz. Experimental results, at their turn, showed maximums of 98.39% for the squares and 98.00% for the hexagons, both at 10.46 GHz. So, results showed that the textile was actually offering a high degree of electromagnetic shielding, increasing the safety for civil and occupational exposures to electromagnetic radiation. In this case, this protection is offered at the microwave frequencies, used especially for telecommunications Earth-satellite which is in the range considered as a potential risk by the WHO (World Health Organization).

Keywords: Electro-textile, wearable, metamaterial, electromagnetic, shielding.

Introduction

The amount of electromagnetic radiation to which humans are exposed is increasing every year due to the use and necessity of wireless applications, since the involved electronic systems and equipments radiate electromagnetic energy in various frequency bands.

High frequency electromagnetic fields above certain levels could trigger biological effects, whereas despite the numerous studies carried out it has not been proven yet that

long exposure to other low-level electromagnetic fields produce any effect on human health [1]. In any case, it has been a huge concern in public health for decades and the World Health Organization (WHO) has been working on it for a long time elaborating several studies and campaigns in order to handle this issue [2].

For this reason, in order to address this international health concern, several methods of electromagnetic shielding have been tried out [3], paying especial attention for those capable of offering constant performance at high degrees of bending (flexibility) and capacity of withstanding humidity while being at the same time light and inexpensive [4].

In order to reach these characteristics, in recent years the application of new conductive textile materials has led to the development of metamaterials (MTMs) in various fields.

A metamaterial is a synthetic composite material with a structure such that it exhibits properties not usually found in natural materials. That is, a class of material engineered and designed to produce properties that do not occur naturally. In addition, these properties are more usually derived from the periodic structure rather than from the components themselves [3]. Although there are different classes of metamaterials the most widely used and the ones that will be considered in this paper are the electromagnetic metamaterials (from now on, for the sake of simplicity referred simply as metamaterials), which exhibits negative electrical permittivity and magnetic permeability, while these values are positive for most of the materials that can be found in nature. Along with these new materials, several new concepts have appeared (Figure 1).

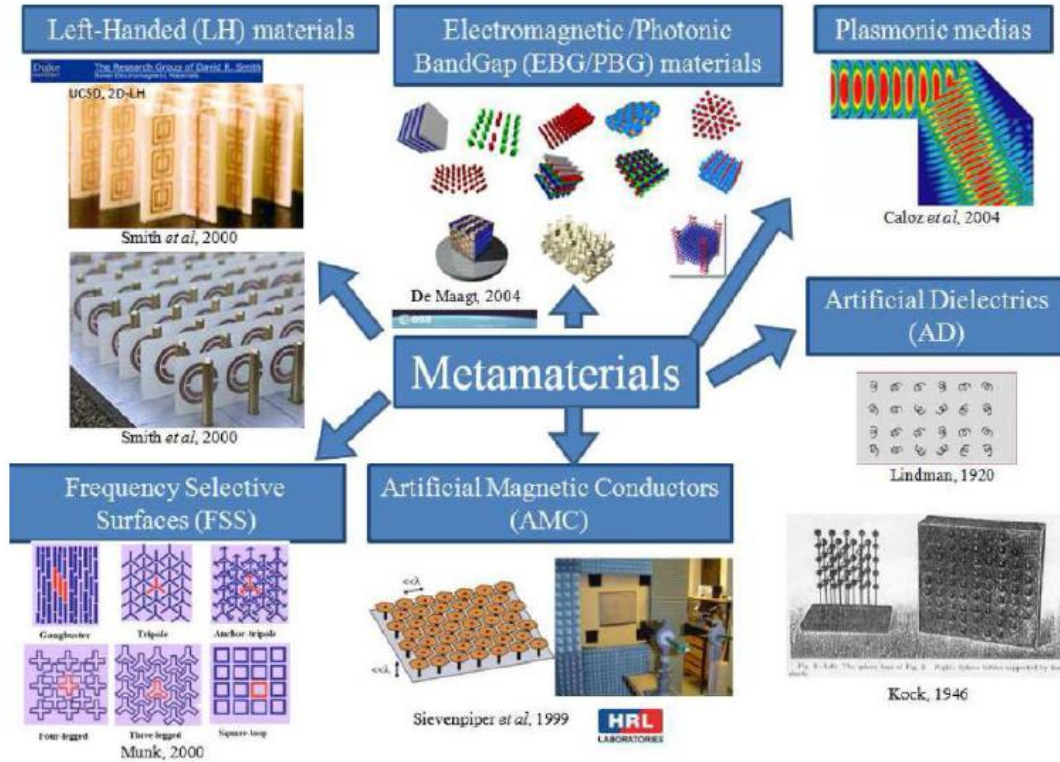


Figure 1. Scheme of existing types of metamaterials [4].

Special attention deserve those whose mission is blocking electromagnetic radiation at certain frequencies and known as Electromagnetic absorbers (EMAs) [5].

Then, in the last years, components using textile materials for wearable applications have become an attractive research topic due to its low cost, ease of fabrication, practicability and low weight [6].

First investigations regarding metamaterials as electromagnetic absorbers were focused on obtaining effective negative permittivity, permeability, and refractive index. These kinds of metamaterials have received especial attention mainly because of their potential applications, including stealth technology and the reduction of automotive false imaging. A very popular solution for thin metamaterials devoted to electromagnetic blocking are the frequency selective surfaces (FSSs) [6].

A frequency-selective surface (FSS) is a structure consisting most typically of two-dimensional periodic elements, where an array of conducting patches act as a

bandstop filter, namely, rejecting waves at the patches resonant frequency but passing them at higher and lower frequencies [7], as depicted schematically in Figure 2. The appropriate selection of FSSs array elements, shape, dimensions and substrate materials are the most important parameters in the design process [8], since these are the parameters that will define both the properties of the surface and the resonance frequency (f_r), which is a result of the impedance and the conductance of the surface [9]. One possible combination for doing this is by using conductive textiles, which are usually made from polymer metal coated yarns, and a nonconductive fabric as a substrate. Since conductive yarns are prone to damage by bending and stretching, it is difficult to manufacture a homogeneous conducting prototype by embroidering with them. This fact, along with the embroidering technique, has to be considered in order to predict the electric performance of wearable metamaterials [10].

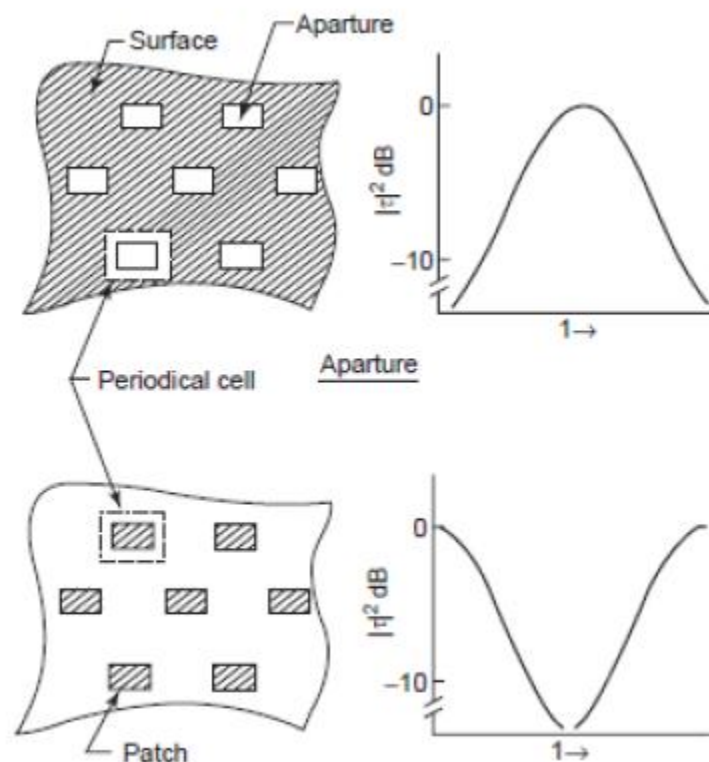


Figure 2. Typical configuration and transmission profile of an FSS [3].

In this work a wearable metamaterial microwave absorber (WMMA) for fixed mobile services and Earth exploration-satellite service [11] is proposed. The prototype WMMA is optimized to reach an absorptivity of almost 100% at its operating frequency using two different unit cells, for comparison.

Simulations of the proposed FSS were performed by using the periodic structure package of the commercial full 3D electromagnetic CST Microwave Studio 2018 software (CST Company, Darmstadt, Germany).

Absorber design, characteristics and simulation

Figure 3 shows the stacking sequence of the layers forming the structure, whereas Figures 4 and 5 depict the geometries of the proposed unit cells. In this paper two different topologies have been tested: square rings and hexagonal rings. The square is the shape that allows most control over the frequency of resonance since his dimensions have a known effect over it. For this reason, the squared shape is the most widely used in general electronic substrates. Hexagons at their turn allow a higher degree of packaging (more unit cells per surface) and that is the reason why they are becoming more and more popular [12,13]. By having these two topologies it is possible to compare both the design strategy and the final results in order to assess the correctness of the procedure and analyse the advantages and the drawbacks of each topology.

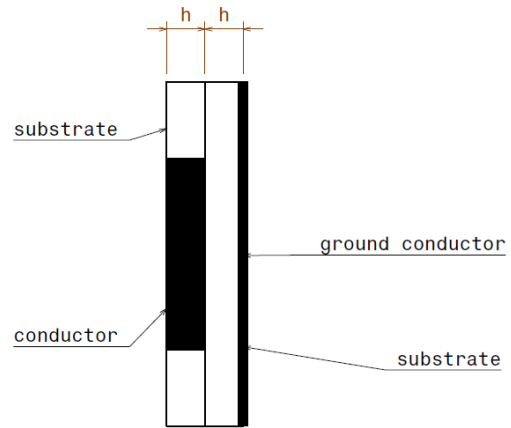


Figure 3. Schematic representation of the disposal of the layers forming the FSS.

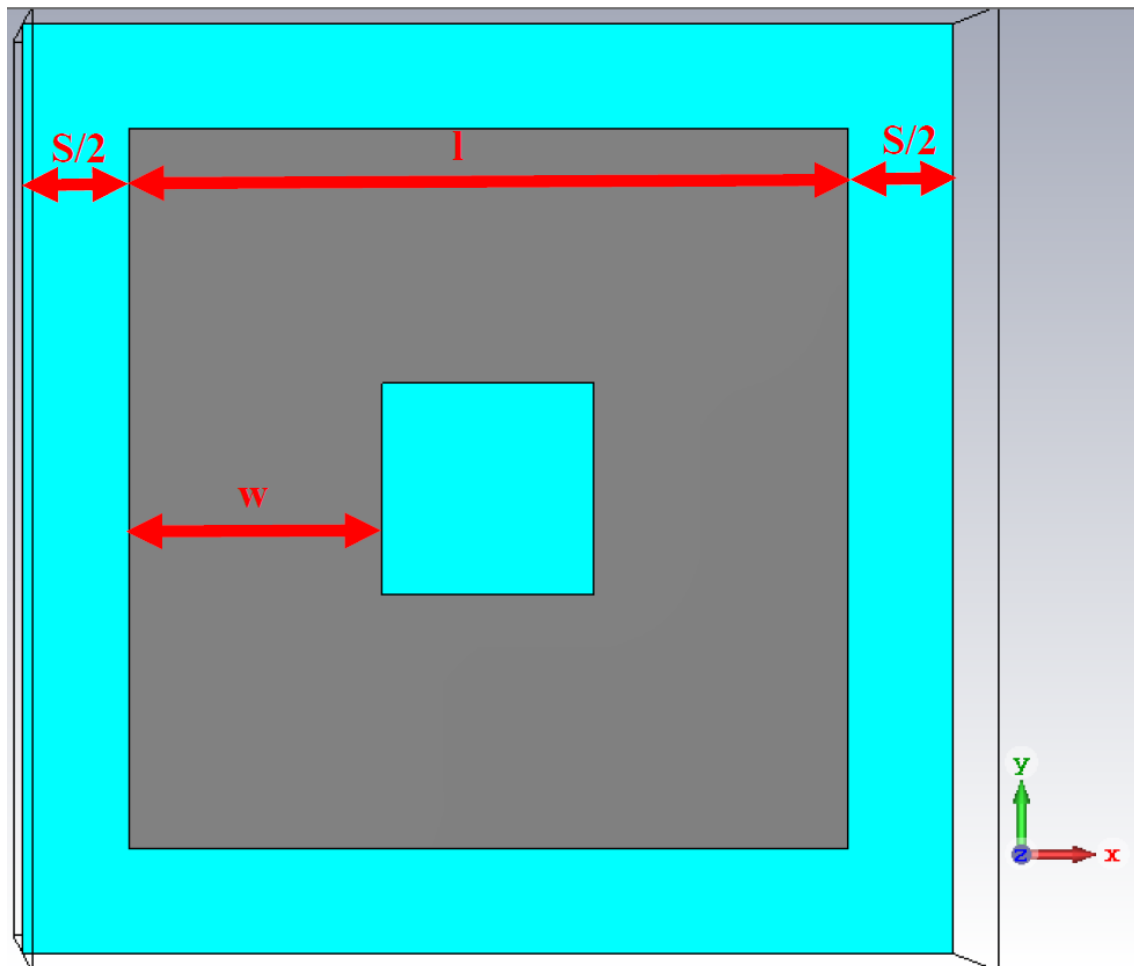


Figure 4. Basic dimensions and parameters used to define the square unit cell.

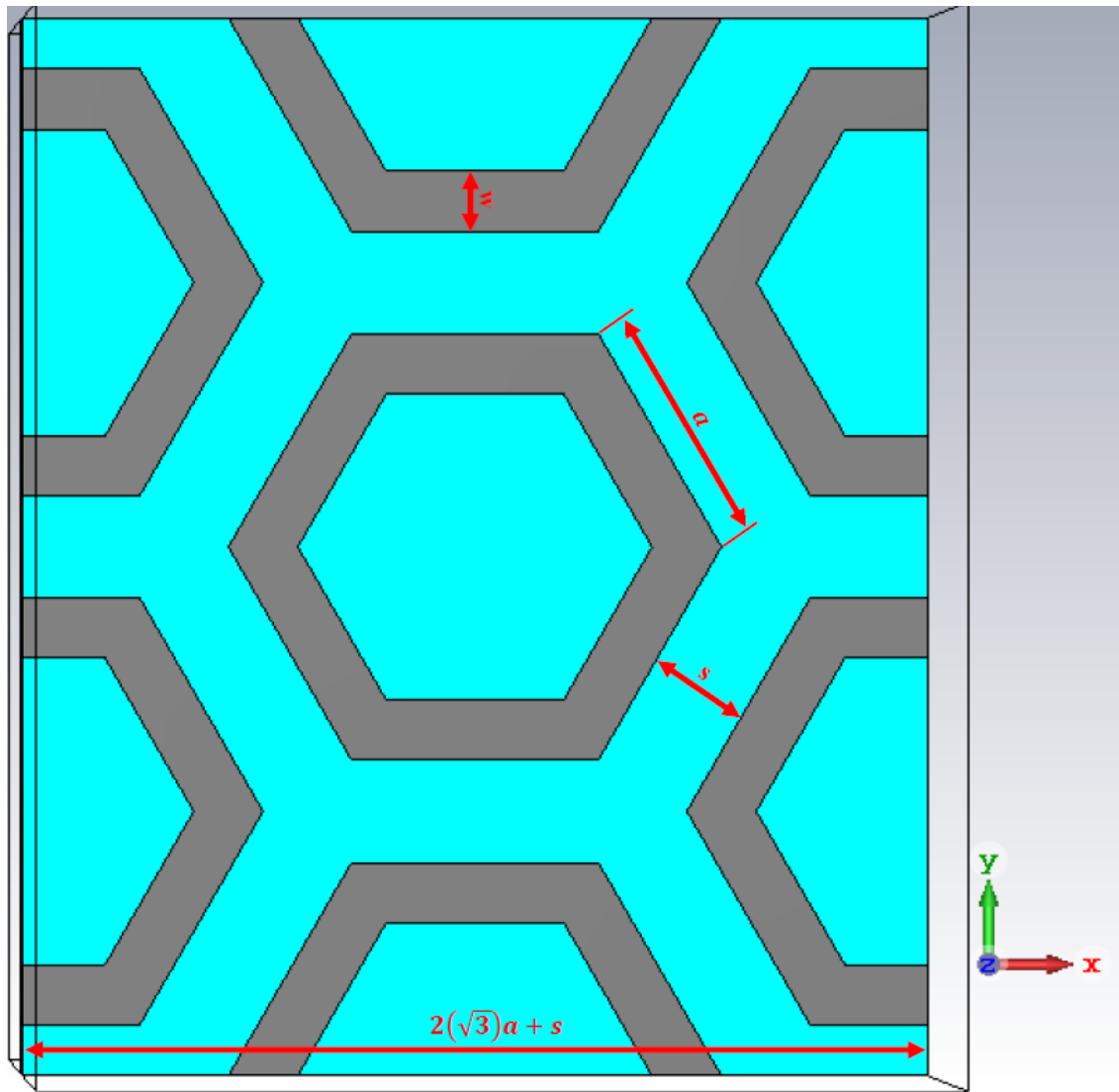


Figure 5. Basic dimensions and parameters used to define the hexagon unit cell.

The first proposed unit cell of the absorber consists of square ring resonators of $l=8.5$ mm, $s=2.5$ mm and $w=3$ mm and hexagonal ring resonators of $a=4.1$ mm, $s=1.7$ mm and $w=1$ mm, a backing ground plane, and a cotton ($\epsilon_r=1.9$, $\tan\delta=0.0580$) substrate with a thickness of $h=0.4$ mm.

The thickness of the substrate is considered a fixed parameter design given by the manufacturer. The other dimensions are obtained by performing a tuning optimization process simulating different geometries around the expected optimal values, up to find the combination that offers the highest absorptivity and widest bandwidth at the desired frequency of resonance, as depicted in Figure 6 as an example for the case of the squares.

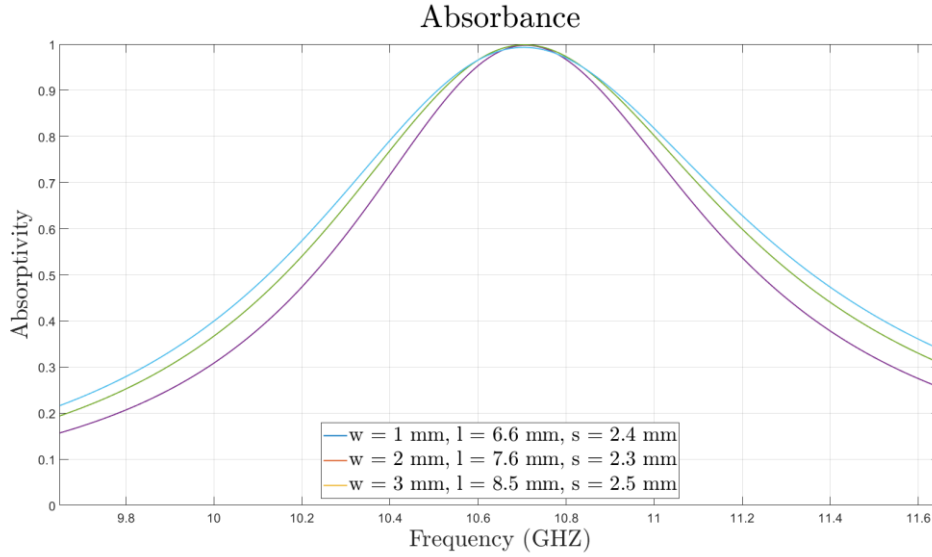


Figure 6. Example of the optimization approach for the square unit cell.

To analyse the performance of the surface, an infinite array approximation is considered and the unit cell is simulated with periodic boundary conditions and Floquet-port excitations. In order to determine the absorptivity, the incident electromagnetic wave (EM) is excited perpendicular to the surface, incident to the face where the arrays are placed. Because of the symmetry and the infinite surface approximation these surfaces are not sensitive to the angle of polarization. The absorptivity $A(\omega)$ of a material is defined as $A(\omega)=1-R(\omega)-T(\omega)=1-|S_{11}|^2-|S_{21}|^2$,

$$A(\omega) = 1 - R(\omega) - T(\omega) = 1 - |S_{11}|^2 - |S_{21}|^2 \quad (1)$$

where $R(\omega)$ and $T(\omega)$ represent the amount of power reflected and transmitted respectively and are related to the scattering parameters (return loss, S_{11} , and insertion loss, S_{21}).

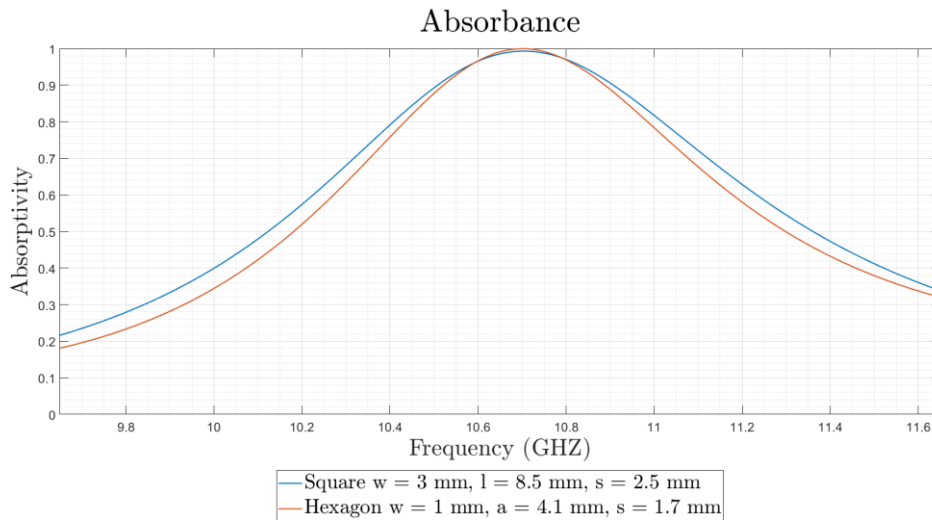


Figure 7. Simulated absorptivity for both the square and the hexagonal unit cell.

In Figure 7 the performance of the different unit cells and their geometrical dimensions are shown. These dimensions are the optimal to achieve the highest absorptivity at the desired frequency of resonance with wider bandwidth. Precision is up to tenths of millimetres since coarser precisions did not allow to reach satisfactory results, whereas more precise dimension would be unrealistic when considering the actual manufacturing processes existing for this kind of embroidered textile structures. Note that, whereas the hexagons present a bit higher peak, the squares are expected to show a wider bandwidth. Finally, in Figure 8 the induced currents at the frequency of resonance in the both types of unit cells are presented, showing the effective impact of the FSS.

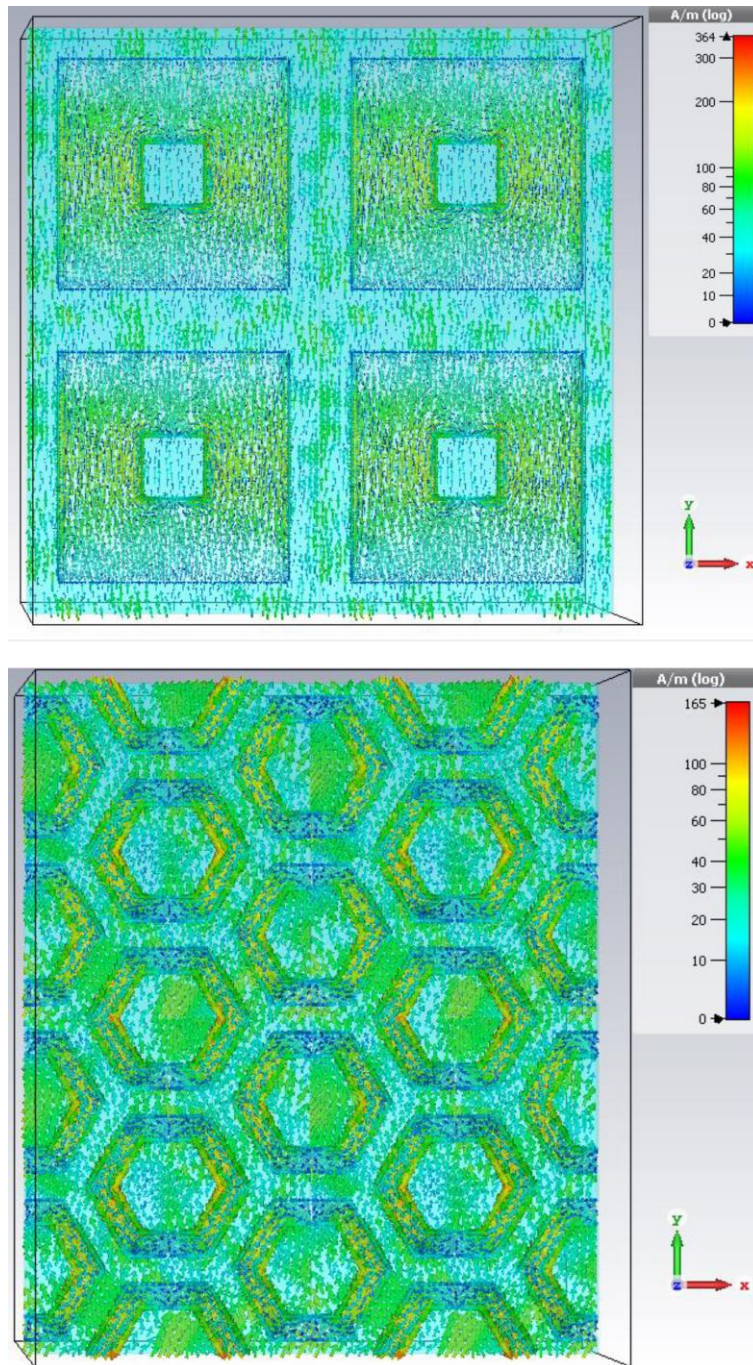


Figure 8. Simulated surface current distributions on the unit cells at resonance frequency.

Manufacturing

Figure 9 illustrates the embroidering process, whereas Figure 10 shows a photograph of the two fabricated WMMA. The used embroidery machine was a Singer Futura XL500, while the selective conductive yarn corresponds to a commercial Shieldex 111/17 dtex-2 ply composed by 99% pure silver-plated nylon yarn 140/17 dtex with a

linear resistance $<30 \Omega/\text{cm}$.

The implemented embroidered pattern was satin with a stitch density of 20% to reduce the overall cost of the FSS. Also, because of the restrictions of the embroidery machine the pattern was stitched with two types of thread: the sulky yarn was used as top thread and the conductive threads were used as bobbin threads. The default value of tension of the higher thread was modified to ensure that it did not break at the same time that geometrical accuracy was kept. The ground bottom layer was made of copper tape, commercial WE-CF adhesive copper sheet (thickness $t = 70 \mu\text{m}$) as depicted in Figure 11.



Figure 9. Process of embroidering the square FSS embroidery structure.

The fabricated prototypes are composed by 196 unit-cells in the case of the squares and 320 for the hexagon-shaped FSS. Note that, as the infinite surface approximation was taken into account in the simulations, the higher the number of unit cells the closer the reality will be to this ideal approximation and, hence, the closer the simulated and the measured results are expected. This phenomenon is due to the intrinsic nature of the metamaterials, whose properties are more related to the structure rather than to the materials itself so, for the induced currents to appear and the blocking

of the radiation at the desired frequency to happen, a significant number of cells must be present.

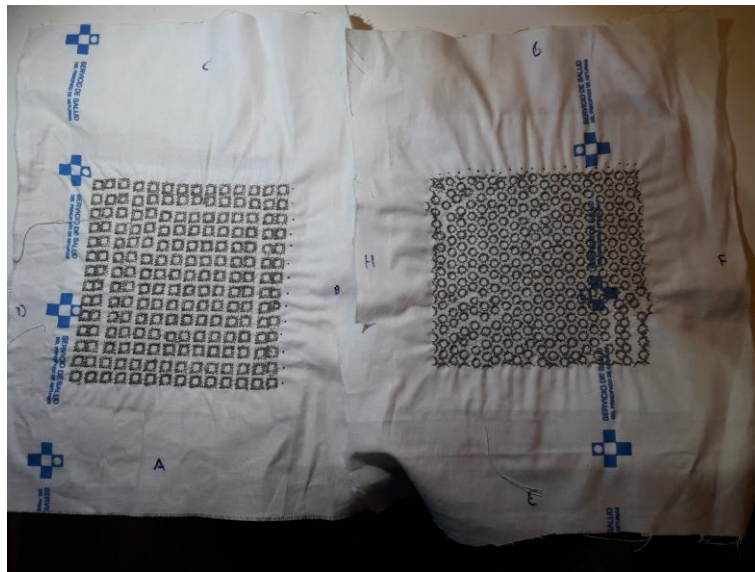


Figure 10. Fabricated FSSs.

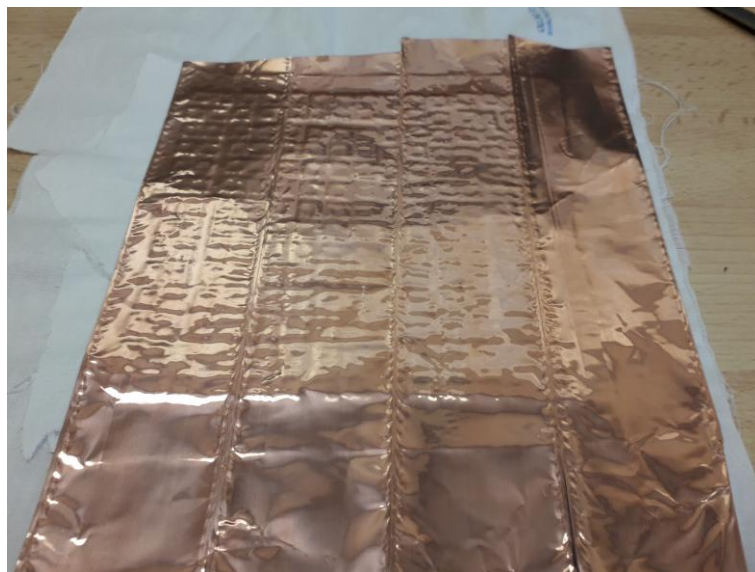


Figure 11. Bottom layer of the fabricated FSS.

Experimental

In order to test the fabricated surfaces an Electromagnetic Diagnostic chamber Rohde & Schwarz DST 200 was used. The different WMMA's were placed inside of it facing downwards to a reference antenna Omnilog 7600, which was used as transmitter, as depicted in Figure 12. The receiver was the antenna already included in the anechoic

chamber. A microwave analyser N9916A FieldFox operating as vector network analyser has been used to determine the corresponding S_{11} parameters for return loss performance and S_{21} for insertion loss. Tested absorptivity is shown in Figure 13.

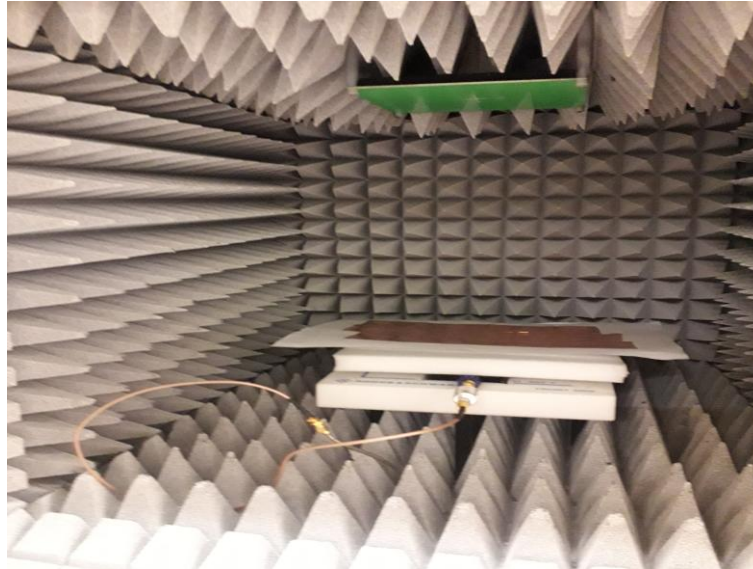


Figure 12. Experimental setup.

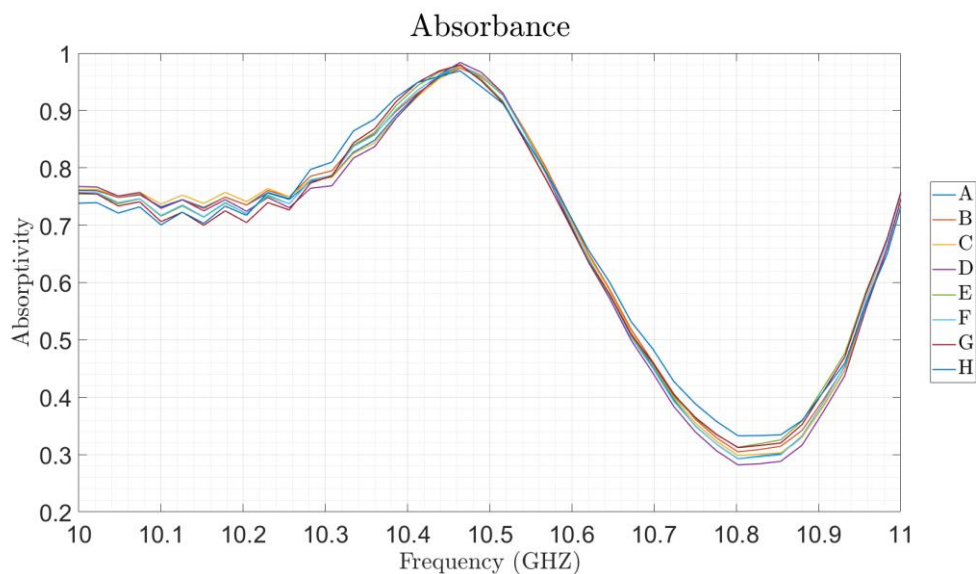


Figure 13. Experimental absorptivity. Letters on Figure 13 refers to the ones shown in Figure 10.

A letter was assigned to each side of the surface to identify them, and both surfaces were tested in the four different possible orientations. Figure 13 allows to appreciate that surfaces were large enough to work properly in all four orientations, since the

results are very similar independently of the orientation. Finally, Figure 14 depicts the detail of the implemented textile FSS.



Figure 14. Detail of the surfaces.

Discussion of the obtained results

When comparing the simulated and the measured results, in Figure 15 it is possible to appreciate how the resonance frequency shifted 0.24 GHz downwards for the tested measures with respect to the simulations, whereas the absorptivity has just decreased around 1% (Table 1).

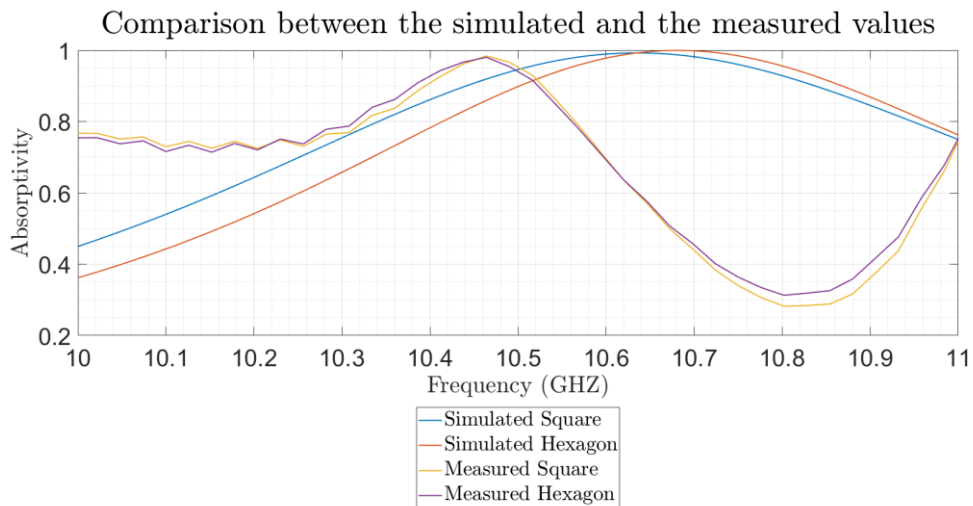


Figure 15. Simulated and measured absorptivity around the frequency of resonance.

Unit Cell	Case	f_r (GHz)	Amax (%)
Square	Simulated	10.63	99.23
Hexagon	Simulated	10.68	99.94
Square	Measured	11.09	95.65
Hexagon	Measured	11.09	94.09

Table 1. Simulated and measured absorptivity.

However, apart from the values of the peak, which are virtually the same, and the small shift in the frequency of resonance, the main difference between the simulated and the measured values is the shape of the curve of absorptivity around the peaks. While the simulated curve follows a continuous trend around the peak, the measured results present in both cases a narrower peak followed by a valley. A common way to assess this difference in band width is to compare the so called FWHM (Full-width at half-maximum), which is the range of frequency between two neighbouring 50% absorption points, and is used as a figure of merit for absorption bandwidth. Then, while this parameter has a value of 0.61 GHz for the simulated squares and 0.56 GHz for the simulated hexagons, the measured values are 0.25 and 0.24 GHz for the tested squares and hexagons respectively, around the half.

Therefore, to sum up, although the maximums of absorptivity reach almost the expected values of 99% the experimental results present a displacement of the frequency of resonance, as well as a decrease in bandwidth and some modulation of the absorptivity curve. These phenomena may be due to different factors, being the most important ones those related with the physical differences between the model and the actual surface. First of all, it has already pointed out that the surface is not infinite as the

simulated one, and also some irregularities and imperfections have appeared on the crafted surfaces because of tolerances in the manufacturing, which is the main cause in the measurement deviations with regard to the simulations. In addition to that, the embroidering technique was not considered on the simulations, which were made considering the conductive parts as solids, instead of inhomogeneous embroidered patterns. Finally, another cause of these differences is the precision of the embroidery machine, which was limited to the order of millimetres, whereas the shapes were defined with a precision up to tenths of millimetre. However, this difference could help explaining the frequency shift but not the difference in shape of the curve, which is more due to the causes previously mentioned. In order to properly understand how each difference between the simulation and the actual surface affected the result it would be necessary to repeat the simulations and tests considering each time one single factor, in order to be able to control their effect or, at least, take them into account when doing the design. However, a much more suitable solution is the use of more complex machinery designed for this purpose actually capable of reaching the desired result, although this would suppose a slight increase in cost. Finally, with a slight retuning of the manufacturing cell embroidery, it is also possible to fit the expected designed results.

Conclusions

An embroidered frequency selective surface for electromagnetic shielding in wearable applications is presented in this paper. The proposed designs correspond with a fully-embroidered conductive thread on a cotton fabric substrate, using two different shapes as unit cell: squares and hexagons. The comparison between the two shapes, as well as between the electromagnetic simulation and measurements were studied, showing a high degree of agreement. The main difference between the simulated and the measured

results was a shift in frequency (around 0.64 GHz) and a decrease of about 50% in the bandwidth of the peak. The maximum value of these peaks, however, was almost the same in both the simulations and the measurements, reaching in both cases values over 98%. Regarding the comparison between the squares and the hexagons very small differences have been appreciated, being the slightly narrower bandwidth (0.24 GHz in front of 0.25 GHz) the only disadvantage found for the squares, although it is not relevant.

The validated results have confirmed that the proposed designs for FSSs are useful for electromagnetic shielding in applications where the use of fabrics is advisable, like in wearable applications.

References:

- [1] Li, Y.Z., Chen, S.H., Zhao, K.F., Gui, Y., Fang, S.X., Xu, Y., & Ma Z.J. (2013, August). Effects of electromagnetic radiation on health and immune functions of operators. *US National Library of Medicine National Institutes of Health*, 31(8), 602-605.
- [2] Radiation and Environmental Health Department of Protection of the Human Environment of the World Health Organization. (2002). *Establishing a dialogue on risk from electromagnetic fields*. Geneva: World Health Organization.
- [3] Inamdar, K., Kosta, Y. P., & Patnaik, S., (2010). Microwave applications of metamaterials concepts. *2010 International Conference on Advances in Recent Technologies in Communication and Computing*, Kettayam, Kerala, India, pp. 292-294. IEEE.
- [4] Naumann, M., Saleem, R., Rashid, A. K., & Shafique, M. F., (2016). A miniaturized flexible frequency selective surface for X-band applications. *IEEE Transactions on Electromagnetic Compatibility*, 58(2):419-428.
- [5] Kshetrimayum, R., (2005). A brief intro to metamaterials. *IEEE Potentials*, 5(23):44-46.
- [6] Tak, J., & Choi, J., (2007). A wearable metamaterial for microwave absorber. *IEEE Antennas and Wireless Propagation Letters*, 16:784-787.
- [7] Wu, Te-Kao. (2005). Frequency selective surfaces. *Encyclopedia of RF and Microwave Engineering*, 10.1002/0471654507.eme133.
- [8] Anwar, R. S., Lingfeng, M., & Ning, H., (2018). Frequency selective surfaces: A review. *Applied Sciences*, 8(9).
- [9] Munk, B. A., (2000). *Frequency Selective Surfaces: Theory and Design*, volume 29. John Wiley & Sons, Inc. Wiley Online Library: Hoboken, NJ, USA, 2000.
- [10] Alonso González, L., (2018). *Design, Simulation and Manufacturing Techniques for Fully Textile Integrated Microwave Circuits and Antennas*. PhD tesis. Universidad de Oviedo: Departamento de Ingeniería Eléctrica, Electrónica, de Computadores y Sistemas
- [11] International Telecommunication Union (ITU). (2007). *Sharing of the 10.6-10.8 GHz band by the fixed and mobile services and the earth exploration-satellite service (passive)*. Technical Report RS.2096.
- [12] Gonçalves Machado, G., Cahill, R., Fusco, V., & Conway, G., (2019). . Comparison of FSS topologies for maximizing the bandwidth of ultra-thin microwave absorbers. In *13th European Conference on Antennas and Propagation*

(EuCAP 2019). IEEE.

- [13] Li, W., & Shamim, A., (2019). Silver nanowires based transparent, broadband fss microwave absorber. In 13th European Conference on Antennas and Propagation (EuCAP 2019). IEEE.